Fractal geometry model for wear prediction

G. Y. Zhou and M. C. Leu
Department of Mechanical and Industrial Engineering, New Jersey Institute of Technology, Newark, NJ 07102 (USA)
D. Blackmore
Department of Mathematics, New Jersey Institute of Technology, Newark, NJ 07102 (USA)

(Received October 6, 1992; accepted February 4, 1993)

Abstract

Fractal characterization of surface topography is applied to the study of contact mechanics and wear processes. The structure function method is used to find the fractal dimension D and the topothesy L. We develop a fractal geometry model, which predicts the wear rate in terms of these two fractal parameters for wear prediction. Using this model we show that the wear rate V_r and the true contact area A_r have the relationship $V_r \propto A_r^{m(D)}$, where $m(D)$ is a function of D and has a value between 0.5 and 1. We next study the optimum (*i.e.* the lowest wear rate) fractal dimension in a wear process. It is found that the optimum fractal dimension is affected by the contact area, material properties and scale amplitude. Experimental results of wear testing show good agreement with the predictions based on the model.

1. Introduction

Wear is a process that involves surface contact, stress action and surface degradation. As a measure of damage to, or material removed from, a solid surface, wear can be considered to be the result of the surface being stressed mechanically, thermally and chemically. The cost of wear in the USA has been estimated to be in the range of tens of billions of dollars per year. There has been constant research effort to gain improved understanding of wear phenomena, to predict wear behavior, and to control wear processes.

When two rough, nominally flat, surfaces are brought together, surface roughness causes contact to occur at discrete contact spots. The true contact area is the accumulation of areas of the individual contact spots. For most metals at normal loads this will be only a few per cent of the apparent contact area [1]. A significant aspect of contact mechanics is that deformation occurs in the region of the contact spots which build up load-related stresses. Typical models of surface deformation are either elastic, plastic or mixed elastic–plastic, depending on nominal pressure, surface topography and material constants.

Fractal geometry as a tool for the characterization of surface topography has gained much attention in recent years [2–4]. This is due in part to the observations that fractal geometry can reflect the natural and intrinsic properties of random phenomena [5–7] and that it can overcome several disadvantages of conventional statistics and random process methods of surface analysis [4]. These advantages suggest, for example, that fractal geometry can be applied to surface contact mechanics. Majumdar and Bhushan explored these applications in a pioneer study [8]. They gave a fractal representation of surface contact area and derived a fractal model of surface contact mechanics. In a recent study [9(a), 9(b)] we developed a fractal model which has a clear connection with conventional statistical methods for studying surface topography. This model leads to a concise quantitative representation of the bearing area curve, and it strongly suggests the applicability of fractal geometry to surface contact and wear process analysis.

The objective of this paper is to establish a fractal model for wear prediction, with which to study the effects of fractal geometry parameters on wear rate. The paper is organized as follows. Section 2 introduces a physical interpretation of fractal geometry in surface characterization, shows the connection of fractal geometry with conventional analysis through the bearing area curve, and develops the structure function technique for obtaining fractal parameters. Section 3 proposes a fractal model for wear prediction which enables us, for the first time, to connect fractal geometry, contact mechanics and wear theory. Section 4 analyzes the variables in the model and provides some useful ideas for wear prediction and control. Based on the model, Section 5 studies optimum fractal dimensions in wear

0043-1648/93/$6.00

processes. Section 6 describes the data of a wear test which provides a qualitative validation of our model. Section 7 contains several conclusions drawn from our study.

2. Characterization of surface topography by fractal geometry

For the sake of completeness, we shall now summarize some basic features of our fractal geometry approach to the study of surface topography. Further details can be found in refs. 9(a) and 9(b).

2.1. Physical interpretation of fractal geometry parameters

Fractal geometry reveals natural properties of random and unpredictable phenomena. The fractal dimension D is the most important aspect of fractals. For different fractal phenomena, the fractal dimension parameter may characterize different properties of fractal sets. For surface topography characterization, fractal parameters can be related to a conventional concept, the normalized bearing area curve. From our modeling of and experiments with fractal surfaces, we concluded (see refs. 9(a) and 9(b)) that, if D increases or the topothesy L decreases, the normalized bearing area curve will shift higher as shown in Fig. 1 and that D has a larger effect on the normalized bearing area curve than L has. The bearing area curve can be viewed as an indicator of contact support ability, where by contact support ability we mean the potential of the surface for establishing sizeable interface areas when in contact with other surfaces. Thus the fractal dimension can represent the bearing area curve used in the conventional analysis for the study of surface contact and wear, and it is more concise and practical since it provides a simple quantitative measure of the contact support ability of surfaces: the larger the fractal dimension value the stronger the contact support ability.

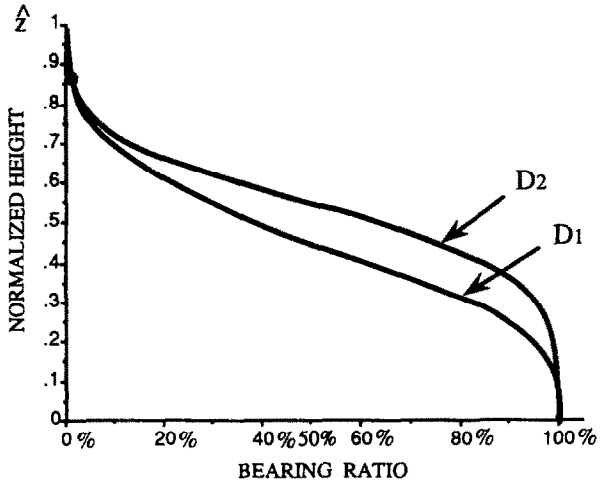

Fig. 1. Normalized bearing area curves for fractal dimensions $D_1 < D_2$.

2.2. Techniques developed for obtaining characteristic parameters of fractal surfaces

Several methods have been developed to characterize the dimension of a fractal set, such as the compass dimension, box dimension, mass dimension and area–perimeter dimension [5, 6]. All of these methods can be easily computed for self-similar fractals. However, it is rather hard to evaluate them for self-affine fractals [10] since these types of fractals are not isotropic. In this study, we are mainly concerned with surfaces which are self-affine. Thus only some special techniques can be readily used to compute fractal dimensions, such as the power spectrum method [4]. If a homogeneous and isotropic rough surface has fractal dimension D_s and its profile in an arbitrary direction has fractal dimension D_p, then a simple relation exists between them; namely, $D_s = 1 + D_p$ [11]. In the experimental part of our study a stylus profilometer was used to measure surface profiles and the acquired data were processed to obtain D_p. The subscript p will be omitted from D_p for simplicity.

We use the structure function method to calculate fractal parameters D and L, because the structure function has a relatively simple mathematical representation and its sampling signal is easy to use for data processing.

Suppose $z(x)$ is a fractal function; it is well known that its correlation $\langle z(x_1)z(x_2)\rangle$ and hence its variance $\langle z^2(x)\rangle$ are infinite, and $z(x)$ is not differentiable. Berry [12] suggested using a structure function to characterize $z(x)$. The increment $z(x+\lambda)-z(x)$ is assumed to have a gaussian distribution with zero mean and the following variance:

$$\langle [z(x+\lambda)-z(x)]^2\rangle = \frac{2C_1}{4-2D}\sin\left[\frac{\pi}{2}(2D-3)\right]\Gamma(2D-3)|\lambda|^{4-2D} \tag{1}$$

where λ is any displacement along the x direction, C_1 is a constant, D is the fractal dimension of the $z(x)$ function and $\Gamma(\ )$ is the gamma function. The variance is called the structure function. It can be seen that the chord joining z values separated by a distance λ has a finite mean-square slope. If there is a displacement $\lambda = L$ such that the chord has an r.m.s. slope of unity statistically, then a concise formula can be written, namely

$$\langle [z(x+L)-z(x)]^2\rangle / L^2 = 1 \tag{2}$$

where L is a characteristic parameter of the fractal function called the topothesy. By comparing eqns. (1) and (2), an equation relating the structure function with fractal geometry parameters is derived:

$$\langle [z(x+\lambda)-z(x)]^2 \rangle = L^{2D-2}|\lambda|^{4-2D} \qquad 1<D<2 \qquad (3)$$

Such a function is both stationary and isotropic. From the above relations D and L can be expressed as

$$D=\frac{4-\beta}{2} \qquad 0<\beta<2 \qquad (4)$$

$$\log L=\frac{C_2}{2D-2} \qquad (5)$$

where β is the slope of eqn. (3) plotted on double logarithmic coordinates and C_2 is the intersection of the structure function curve with the y axis.

Figure 2(a) shows three electric discharge machining (EDM) specimens which have different surface features that lead to different fractal dimensions. Figure 2(b) shows the log–log plots of structure functions which can be used to calculate the fractal dimensions of these three surfaces. It can be seen that they all have straight slopes along major portions of their curves. These observations strongly suggest that the structure function is an effective method for finding D and L of self-affine fractal sets.

Note that in our calculations we assume that the shortest wavelengths of a Weierstrass–Mandelbrot model of the surface profile are tribologically dominant and that the structure function can be extrapolated to arbitrarily short wavelengths in order to obtain the intercept used to compute L. Both of these assumptions are intuitively plausible in view of the postulated self-affine fractal character of the surface, and they are in accord with the approach taken by Thomas and Thomas [13].

3. Fractal geometry and wear theory

In this section, by using the same fractal approach as that developed by Majumdar and Bhushan [8] in the study of surface contact mechanics, we develop a fractal model for surface wear processes. This model reveals interesting relationships between wear characteristics and fractal parameters.

3.1. Fractal property of islands

It has been shown by Archard [14], Mandelbrot *et al.* [11] and Majumdar and Bhushan [4] that the microtopography of some machined surfaces is similar to a map of the Earth's surface, which has islands in the various bodies of water. When a rough surface is in contact with a flat surface, the flat surface (like an ocean in the formation of islands on the Earth) cuts the rough surface and forms the contact area. This island analogy has been successfully used to study contact mechanics (*e.g.* in ref. 8), and we shall therefore employ it to analyze wear. Korcak [15] proposed an empirical law which can be described as follows. If all the islands of a region are listed by size, then the total number N of islands of size A exceeding S satisfies the following relation:

$$N(A \geqslant S)=C_3 S^{-B} \qquad (6)$$

where C_3 is a positive constant and B is a factor shown by Mandelbrot [5] to be $B=D/2$, where D is the fractal dimension of the coastlines of the islands. Based on eqn. (6) it can be derived [8] that the total area of all islands A_r can be expressed in terms of the fractal dimension as follows:

$$A_r=\frac{D}{2-D}S_L \qquad 1<D<2 \qquad (7)$$

where S_L is the area of the largest island.

3.2. Fractal relation of contact spots and asperities

The Weierstrass–Mandelbrot function can be used to simulate a fractal surface profile and has the form [4, 16]

$$z(x)=G^{D-1}\sum_{n=n_1}^{\infty}\frac{\cos(2\pi\eta^n x}{\eta^{(2-D)n}} \qquad 1<D<2,\ \eta>1 \qquad (8)$$

where η is a frequency factor, n is an integer, n_1 is the minimum of n which is determined by the measuring length, and G is a factor called the scale amplitude by Majumdar and Bhushan [4]. It can readily be shown that $L=C_4G$, where C_4 is given by the formula

$$C_4=\left\{\frac{\Gamma(2D-3)\sin[\pi(2D-3)/2]}{2-D}\right\}^{1/(2D-1)} \qquad (9)$$

Here the gamma function Γ denotes the analytic continuation of the usual integral $\int_0^\infty t^{z-1}e^{-t}\,dt$ to a meromorphic function on the complex plane which has simple poles at all the non-positive integers. Note that $\Gamma(x)$ has a singularity of the form $1/ex$ as $x\to 0$, so $\sin(x)\Gamma(x)$ is not singular at $x=0$. Hence the right-hand side of eqn. (9) is a continuous function of D for $1<D<2$. For a given surface the fractal dimension D is a fixed number, and hence C_4 is a constant. Thus we see that G is directly related to the topothesy L.

It has been shown [8] that the critical area S_c that distinguishes the elastic and plastic regimes can be expressed as

$$S_c=\frac{G^2}{(Q\sigma_y/2E)^{2/(D-1)}} \qquad (10)$$

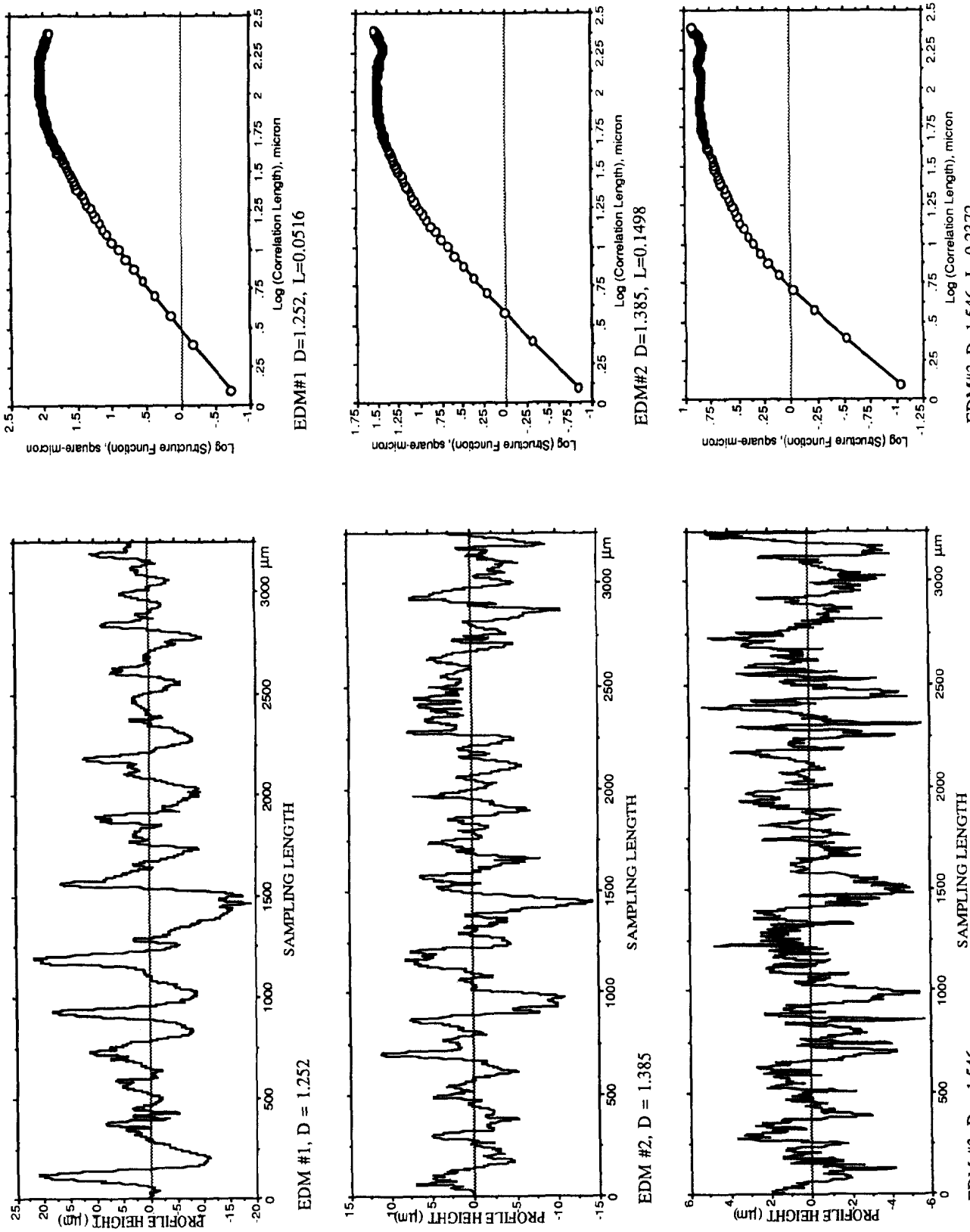

Fig. 2. (a) Three EDM surfaces made with different process parameters. (b) The structure function graphs of the EDM surfaces 1, 2 and 3 in (a).

where σ_y is the yield strength, E is the elastic modulus and Q is a factor that relates the hardness H to the yield strength σ_y as $H=Q\sigma_y$.

If $S_L > S_c$, the real areas of contact in both elastic and plastic deformations need to be considered, and from ref. 8 these contact areas are respectively

$$A_{re} = \frac{D}{2-D}(S_L - S_L^{D/2} S_c^{(2-D)/2}) \tag{11}$$

$$A_{rp} = \frac{D}{2-D} S_L^{D/2} S_c^{(2-D)/2} \tag{12}$$

3.3. Adhesive wear theory

There exist many wear theories such as adhesive, abrasive, fatigue, corrosion and delaminative theories [14, 17–19]. The origin of all these is Archard's adhesive wear theory [17]. Archard's adhesive wear theory has been widely accepted and utilized (*e.g.* in refs. 20 and 21), since the derived relationship among the wear volume, sliding distance and contact area has been observed to agree well with experimental results. The mechanism of adhesive wear is consistent with our experiment of wear testing, and so we shall use it as the starting point of wear analysis which follows.

Adhesive wear can be described as follows: materials weld at sliding asperity tips, are transferred to the harder member, possibly grow in subsequent encounters, and are eventually removed by fracture, fatigue or corrosion. It is shown in ref. 17 that adhesive wear can be expressed in the form

$$V = KA_c d \tag{13}$$

where V is the wear volume, K is a wear coefficient, A_c is the true contact area, and d is the sliding distance. The true contact area A_c has the relation $A_c = W/p$, where W is the normal load and p is the normal pressure. According to Tabor [22] wear occurs when the normal stress p and the shear stress s have the following relation:

$$p^2 + \gamma s^2 = p_m^2 \tag{14}$$

where p_m is the yield pressure and γ is an experimentally determined constant which relates to material hardening, lubricant, material interfacing, ploughing etc. The value of γ can range between 3 and 25 (Tabor assumed that γ has a value of about 9).

Equation (14) indicates that once the summation of p^2 and γs^2 reaches p_m^2 the plastic flow will occur. When there is only a constant normal load W which acts on a pair of contact surfaces and plastic flow occurs, the true contact area A_c has the relation $A_c = W/p$. As discussed in Tabor's paper [22] when a tangential force F is applied there are both normal and shear stresses on the surface. The shear stress produces a finite displacement at the interface. As a result the area of contact increases. Thus the normal pressure p required for producing plastic flow decreases. If the shear stress is big enough then the combined effect of p and s is still capable of producing plastic flow in the interface. This means that when s is increasing p will decrease and the contact area will become large. Based on eqn. (13), the larger the true contact area the larger the wear volume.

The adhesive theory of friction (see ref. 22) leads to the expression

$$s = \frac{\mu W}{A_c} = \frac{T}{A_c} = \mu p \tag{15}$$

where T is the total friction force and μ is the coefficient of friction. Substituting eqn. (15) into eqn. (14) yields

$$p = \frac{p_m}{(1+\gamma\mu^2)^{1/2}} \tag{16}$$

The wear equation now becomes

$$V = K(1+\gamma\mu^2)^{1/2} A_r d \tag{17}$$

where $A_r = W/p_m$ is the true contact area under static loading.

As mentioned above, the model of surface deformation usually involves a combination of elastic and plastic effects. It is reasonable to assume that the total true contact area A_r is the sum of the elastic contact area A_{re} and the plastic contact area A_{rp}, *i.e.*

$$A_r = A_{re} + A_{rp} \tag{18}$$

This leads to the following wear volume equation:

$$V = (1+\gamma\mu^2)^{1/2}(K_e A_{re} + K_p A_{rp}) d \tag{19}$$

where K_e and K_p are the elastic and plastic wear coefficients respectively.

Notice that in eqn. (19) the wear coefficient K has been decomposed into elastic and plastic components. It was pointed out by Archard [14] and Stolarski [20] that, if the deformations are completely plastic, then K is essentially a probability coefficient which represents the cumulative effects of lubrication, sliding speed, temperature, chemical reactions, material properties etc., and K is independent of the topographies of the surfaces which are in contact. For example, if $K = 10^{-3}$ in a completely plastic wear process, then one in 1000 events results in a worn particle. It was, however, observed by Archard [14] that an actual wear process also includes elastic deformations, and this will introduce a surface-topography-dependent element to K, *i.e.* K becomes an A_r-dependent coefficient rather than a constant. By decomposing K into elastic and plastic parts, the coefficient K is replaced by the coefficients K_e and K_p, both of which are independent of the geometric features of the contacting surfaces. Thus K_e

and K_p can be treated as probability constants. According to Archard's investigations, K varies widely, from 10^{-7} to 10^{-2} in unlubricated wear. If the deformations are completely plastic, the maximum value of K_p is 1/3. The value of K_e in most wear processes is less than 10^{-3}.

4. Wear prediction model and analysis

Here we shall develop a model that relates wear to fractal parameters. By substituting eqns. (11) and (12) into eqn. (19), the wear volume becomes

$$V=(1+\gamma\mu^2)^{1/2}S_L[K_e(1-S_L{}^{(D-2)/2}S_c{}^{(2-D)/2}) + K_pS_L{}^{(D-2)/2}S_c{}^{(2-D)/2}]d \tag{20}$$

With eqns. (7) and (10), eqn. (20) can be rewritten as

$$V=(1+\gamma\mu^2)^{1/2}A_r\left\{K_e-(K_e-K_p)\times\left[\frac{D}{(2-D)A_r}\frac{G^2}{(Q\sigma_y/2E)^{2/(D-1)}}\right]^{(2-D)/2}\right\}d \tag{21}$$

For ease in analysis, we normalize the variables in eqn. (21) as follows:

$$V^*=\frac{V}{dA_a}$$

$$A_r{}^*=\frac{A_r}{A_a}$$

$$G^*=\frac{G}{A_a{}^{1/2}} \tag{22}$$

$$\psi=\frac{Q\sigma_y}{2E}$$

where A_a is the apparent contact area; V^* is the normalized wear rate; $A_r{}^*$ is the normalized true contact area; G^* is the normalized scale amplitude; and ψ is a material property constant. With the normalized variables, eqn. (21) can now be rewritten as

$$V^*=(1+\gamma\mu^2)^{1/2}A_r{}^*[K_e-(K_e-K_p)]\times\left[\frac{D}{(2-D)A_r{}^*}\frac{G^{*2}}{\psi^{2/(D-1)}}\right]^{(2-D)/2} \tag{23}$$

We call this the fractal geometry model of wear prediction. With eqn. (23) the wear rate V^* can be evaluated as a function of $A_r{}^*$, D, G^* and ψ.

If the area of the largest contact spot S_L is less than the critical area of plastic deformation, *i.e.* $S_L<S_c$, then only plastic deformation will take place. In that case $K_e=0$ in eqn. (23).

A few remarks are in order concerning eqn. (23). Our equation treats both the plastic and elastic aspects of wear together. This is not to suggest that both plastic and elastic wear are of equal magnitude at each instant of the wear process. We emphasize that eqn. (23) is a dynamic equation in which D, G and the other parameters vary during the wear cycle. At the start of the entire process, the plastic wear is dominant. As the process continues with D and G changing, the dominance of the plastic mode subsides and the elastic component becomes a more significant contributor to the total mechanism of wear. In our wear experiments (described in Section 6) the fractal parameters are measured at various times during the wear process in order to test for a correlation between the changes in the fractal geometry and changes in the stages of wear. We note that ergodicity of the surface was not assumed in the derivation of eqn. (23). In fact, we showed in refs. 9(a) and 9(b) that a self-affine fractal model for the surface topography leads to a non-stationary random process which is not ergodic.

4.1. *Effect of fractal dimension on wear rate*

The effect of fractal dimension on wear rate is a major concern. To investigate numerically how V^* is affected by D using eqn. (23), the values of other parameters need to be chosen. Based on the literature [4, 9(a), 14, 20], for ordinary cases the parameter values may be chosen as $G^*=10^{-9}$, $\psi=0.01$, $\mu=0.2$, $\gamma=9$, $K_e=10^{-4}$ and $K_p=0.1$. In Fig. 3 $\log V^*$ is plotted against $\log A_r{}^*$ for various D values. It can be seen that there are two regions of D that have significantly different wear rate behavior. In the first region, for D between 1.15 and 1.5, V^* decreases with increasing D. In the

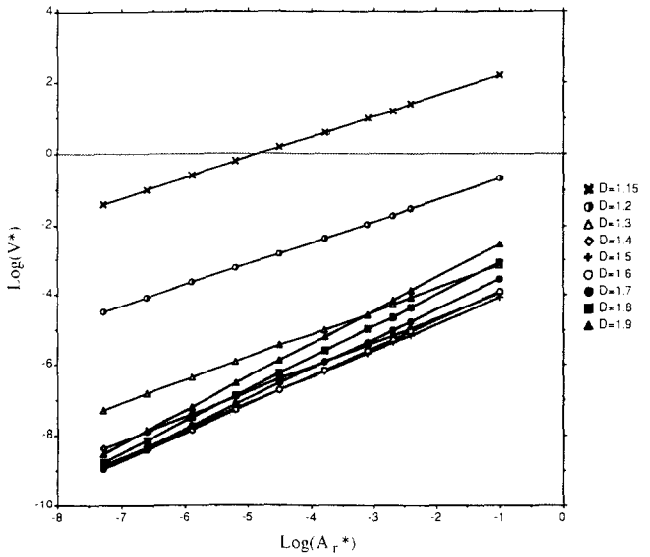

Fig. 3. Effect of fractal dimension D and normalized contact area $A_r{}^*$ on normalized wear rate V^*.

second region, for D between 1.6 and 1.9, V^* increases slightly with increasing D. To show this more clearly, the relations in these two regions are plotted separately in Figs. 4 and 5. Figure 4 shows that, when D increases, V^* decreases and that this relationship is non-linear. When D increases from 1.15 to 1.2, an increase of D by only 0.05, V^* decreases by an average of 3.2 decades for the range of A_r^* considered. When D increases from 1.2 to 1.3, V^* decreases by 2.5 decades. As D increases from 1.3 to 1.4 and from 1.4 to 1.5, the decreases in V^* are 1.2 decades and 0.5 decades respectively. Figure 5 shows that V^* increases with increasing D for the range of D between 1.6 and 1.9.

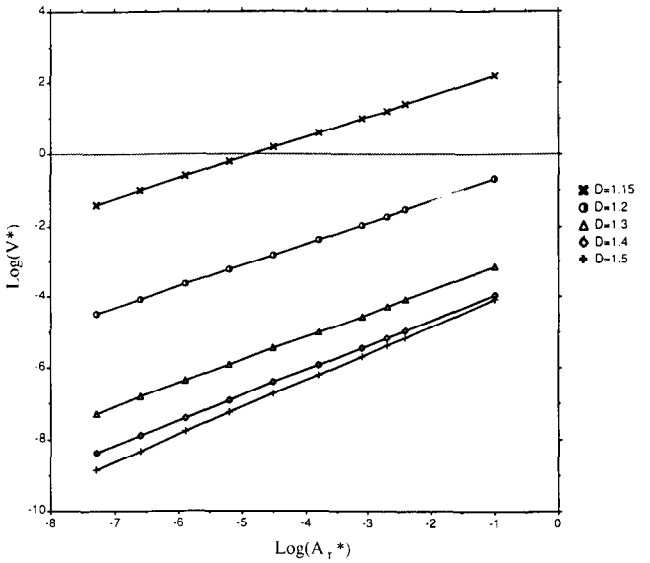

Fig. 4. The V^*–A_r^* relation for the first range of fractal dimension D values: 1.15–1.5.

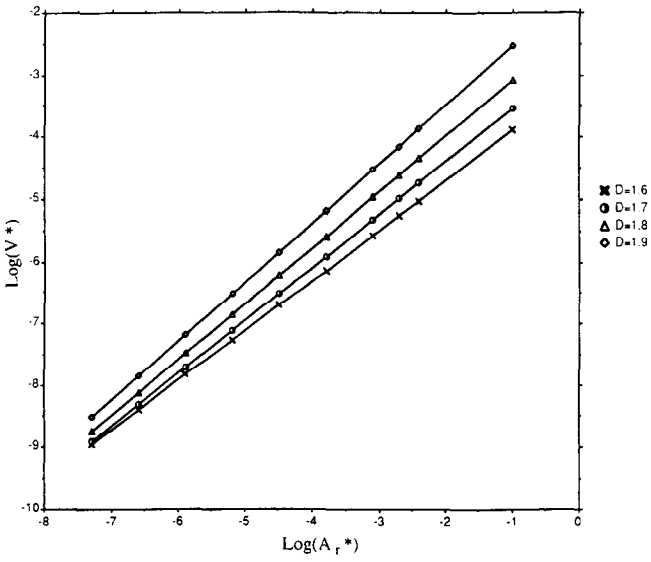

Fig. 5. The V^*–A_r^* relation for the second range of fractal dimension D values: 1.6–1.9.

This wear rate behavior in the two fractal dimension regions can be explained as follows.

When D increases from 1.15 to D_m, which is approximately 1.5 for the chosen parameter values and later in Section 5 will be called the optimum fractal dimension, there is a corresponding upward shift of the bearing area curve which signals an increase in the surface contact area. Consequently, the normal contact pressure between the surfaces under the same load decreases with increasing D; thus the wear rate decreases. However, the rate of upward shift in the bearing curve decreases as D approaches D_m from the left, which is in accord with the prediction of the fractal surface model developed in refs. 9(a) and 9(b). One possible explanation of the subsequent increase in the wear rate as D assumes values in excess of D_m is as follows. The rate of upward shift in the bearing area curve is small when $D > D_m$. Over the wear process, an accumulation of worn material occurs between the surface and the number of asperities per unit surface area increases with the tips of the asperities becoming sharper and weaker. The net effect is a rather substantial increase in the topothesy which tends to lower the bearing area curve. It may be that the increase in L becomes sufficient to overcome the effect on the contact support ability due to increasing D, so that there occurs a very small downward shift of the bearing area curve in the interval $(D_m, 2)$ and a consequent increase in the wear rate.

The above observations can be summarized as follows. For a fractal surface with $1 < D < D_m$, the contact support ability is dominated by the size of D; but when $D > D_m$ other factors such as the growth of L tend to exert more influence on the wear rate than D.

It should be noted that the value of D_m that distinguishes the two regions of wear rate behavior may vary for different wear parameter values. For example, the D_m value is about 1.7 for the wear material and process described in Section 6.

4.2. Dependence of wear rate on true contact area under static loading

From Fig. 3 it can be seen that, for every D, log V^* increases linearly with log A_r^*, since each plot is a straight line on the log–log graph. In Archard's equation, the wear rate $V_r = V/d$ is proportional to the true contact area under static loading, i.e. $V_r \propto A_r$. As he pointed out in ref. 14 this relationship was based on the assumption that all deformations are plastic and that the asperities are isolated. However, if all deformations are elastic and the asperities are isolated, the wear rate should satisfy the relation $V_r \propto A_r^{2/3}$ (see ref. 14). If deformations are mixtures of elastic and plastic deformations and the asperities are not isolated, the wear rate can be expected to have the relation $V_r \propto A_r^q$,

where q is an undetermined constant which is related to the surface topography.

In the wear prediction model of eqn. (21), we have included both elastic and plastic deformations. It is possible to use this equation to predict the power q in the relation $V_r \propto A_r^q$. Rewrite eqn. (21) as follows:

$$V_r \propto K_e A_r - j(K_e - K_p) A_r^{D/2} \tag{24}$$

where

$$j = \left[\frac{D}{2-D} \frac{G^2}{(Q\sigma_y/2E)^{2/(D-1)}} \right]^{(2-D)/2} \tag{25}$$

For a typical case encountered in engineering practice, $D = 1.5$, $G = 10^{-7}$ m, $Q\sigma_y/2E = 0.001$ (for steel material), $K_e = 10^{-4}$ and $K_p = 0.1$; then $j = 0.42$ and eqn. (24) can be estimated as

$$V_r \propto 10^{-4} A_r - (0.42 \times 10^{-4} A_r^{D/2}) + 0.042 A_r^{D/2} = A_r^{m(D)} \tag{26}$$

or

$$V_r \propto A_r^{m(D)} \tag{27}$$

where $m(D) \approx D/2$ (note that the other terms in A_r in eqn. (26) are extremely small) is a monotonically increasing function of D and has a value approximately between 0.5 (when $D = 1$) and 1 (when $D = 2$). Once the fractal dimension of a surface is given, $m(D)$ can be determined. By checking the slope of log V^* *vs.* log A_r^* for each D in Fig. 3, it is found that these slopes are between 0.6 (when $D = 1.15$) and 0.94 (when $D = 1.9$). These slopes match with our estimation in eqn. (27). Additional confirmation of this fractal power proportionality can be found in the experimental results provided by Archard [17] about "wear rate over load graphs for brass and stellite pins rubbing on tool steel rings". Because in the adhesive wear theory the true contact area has a relation with the normal load as $A_r \propto W$, these experimental results can also be used to detect the relation between wear rate and true contact area. Based on these experimental results, for brass material the relation is $V_r \propto A_r^{0.98}$ and for stellite it is $V_r \propto A_r^{0.92}$. This is consistent with our predicted fractional power proportionality. These data support the validity of our model and, in so doing, demonstrate the role which fractal geometry can play in the analysis of wear processes.

4.3. *Effect of other parameters on wear rate*

The effect of the scale amplitude on wear rate predicted by our model can be observed from Fig. 6. When G^* increases from 10^{-12} to 10^{-6} (with D fixed at 1.5 and the other parameters having the same values as before), V^* increases monotonically with G^*. This indicates that a larger surface scale amplitude leads to greater plastic deformation wear.

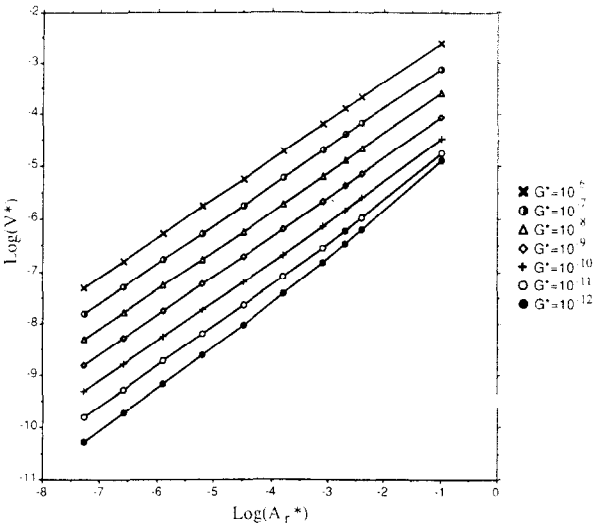

Fig. 6. Effect of scale amplitude G^* on normalized wear rate V^*.

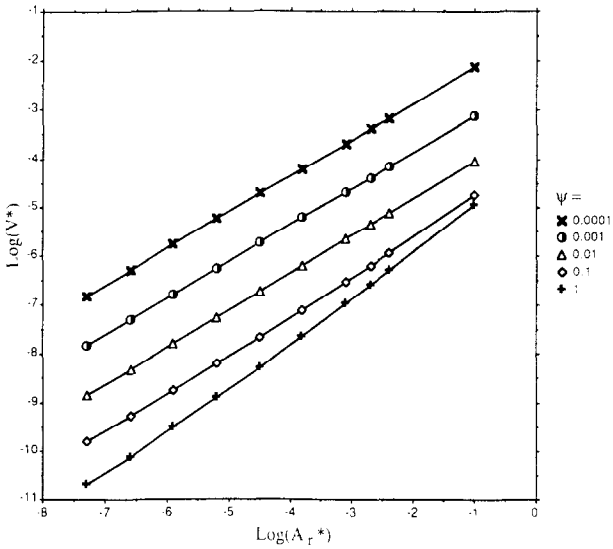

Fig. 7. Effect of material constant ψ on normalized wear rate V^*.

The effect of the material constant ψ on V^* is shown in Fig. 7. It can be seen that V^* decreases with increasing ψ (between 0.0001 and 1). This can be explained by the fact that the hardness of material increases with increasing ψ.

5. Optimum fractal dimensions of wear processes

For a surface in a wear process, the most important requirement is low wear rate. Fractal dimension has been shown to be related to surface contact support ability and wear rate via our model discussed above.

The fractal dimension of the lowest wear rate is of considerable significance in any wear process. The optimum fractal dimension can be found by differentiating eqn. (23) with respect to D and setting it to zero, *i.e.*

$$\frac{dV^*}{dD} = (1+\gamma\mu^2)^{1/2} A_r^* (K_p - K_e) \times \left[\frac{DG^{*2}}{(2-D)A_r^* \psi^{2/(D-1)}}\right]^{(2-D)/2} \times \left[\frac{1}{2}\ln\left(\frac{2-D}{D}\frac{A_r^*}{G^{*2}}\psi^{2(2D-1)/(D-1)^2}\right) + \frac{1}{D}\right] = 0 \quad (28)$$

From our prior discussions there exist $A_r^* \neq 0$, $K_p \neq K_e$, $G^* \neq 0$ and $1 < D < 2$, so eqn. (28) leads to

$$\frac{1}{2}\ln\left(\frac{2-D}{D}\frac{A_r^*}{G^{*2}}\psi^{2(2D-1)/(D-1)^2}\right) + \frac{1}{D} = 0 \quad (29)$$

This is a non-linear equation, and solutions for D are functions of three variables: $D = F(A_r^*, \psi, G^*)$. Thus we see that the optimum fractal dimension depends on the true contact area, material property constant and scale amplitude.

Let us look more closely at eqns. (28) and (29). First, we observe that solving eqn. (29) for D is equivalent to solving

$$D = \phi(D) = (R^*)^{-1}(2-D)e^{2/D}\psi^{2(2D-1)/(D-1)^2} \quad (30)$$

where $R^* = G^{*2}/A_r^*$ and e is the base of the natural logarithm. It is easy to see that ϕ is a strictly decreasing function of D on the interval $1 < D \leqslant 2$ such that $\phi(2) = 0$ and $\phi(D) \to \infty$ as D approaches 1. We conclude therefore that eqn. (30) has a unique solution, say $D = D_m$, in the interval $1 < D \leqslant 2$ which corresponds to the intersection of the line $y = D$ with the curve $y = \phi(D)$.

Referring back to eqn. (28), it can be readily shown that $dV^*/dD < 0$ for $1 < D < D_m$ and $dV^*/dD > 0$ when $D_m < D \leqslant 2$. Hence the minimum value of V^* on $1 < D \leqslant 2$ is attained at $D = D_m$, so D_m is the optimum value of the fractal dimension. Since it is not possible to obtain a closed-form solution of eqn. (30), it is necessary to use numerical methods to obtain values of D_m.

To find the optimum dimension D for various values of A_r^*, Fig. 8 is obtained by replotting Fig. 3. It can be seen from this figure that for different A_r^* values the optimum D values are different, but they are all roughly in the range 1.45–1.55. The effect of the material constant ψ on the optimum dimension can be found by comparing Figs. 8, 9 and 10 which have values of ψ equal to 0.01, 0.1 and 0.001 respectively. In Fig. 9 ($\psi = 0.1$), the optimum values of D for the various A_r^* values are in the range 1.33–1.4. In Fig. 10 ($\psi = 0.001$), the optimum dimensions are in the range 1.58–1.71. All three figures show the same tendency of D as A_r^* decreases from 0.5 to 10^{-6}: the optimum D shifts to a higher value as A_r^* decreases. Also, the figures show that the value of optimal D decreases as ψ increases.

The influence of G^* on the optimum fractal dimension can be seen by comparing Figs. 8, 11 and 12. The optimum D values are around 1.5, 1.55 and 1.45 for the G^* values of 10^{-9}, 10^{-8} and 10^{-10} respectively. The value of D increases as G^* increases.

6. Implementation in wear testing

In this section we present our wear testing results to support qualitatively our fractal model for wear prediction. In our wear testing experiments the wear mechanism [23] consisted of an alloy steel roller (rotating part) and an ion-nitriding treated shoe (fixed part). When the testing was performed, a load was exerted on the mating surfaces and the wear rate was measured periodically. During the wear process the fractal dimensions of the roller and shoe were obtained using the method of surface topography measurement described in ref. 24. The fractal dimensions of four pairs of rollers and shoes were calculated in the experiments and they had very similar values.

The histogram of the wear rate from one of our experiments is shown in Fig. 13. It can be seen from the figure that during the first 30 min of testing the wear rate was fairly high, and then decreased and stayed at a very low rate until 120 min had elapsed; after this time the wear rate increased dramatically. These observed changes of wear rate are consistent with the well-known three stages of a wear process; run-in, mild wear and severe wear, and they can be explained as follows. At the beginning of the wear process the two contact surfaces were fresh and they had very sharp peaks. When they interacted with each other, the sharp layers were worn off gradually. So in this stage (the run-in stage) the wear rate was a little higher than that in the subsequent stage. After the first stage the surfaces became smoother and thus had a larger contact area and a smaller contact stress. This resulted in a stable and very low wear rate. This is the second stage (the mild wear stage) which was between 30 and 120 min. The third stage (the severe wear stage) occured after 120 min. In this stage there existed large shear and normal stresses on the contact surfaces because of thermal, molecular and physical actions. The surfaces became rougher and rougher, and this led to a significant increase in wear rate as the process continued.

The changes of fractal dimensions associated with the above testing are given in Figs. 14(a) and 14(b) for the roller and shoe respectively. During the first

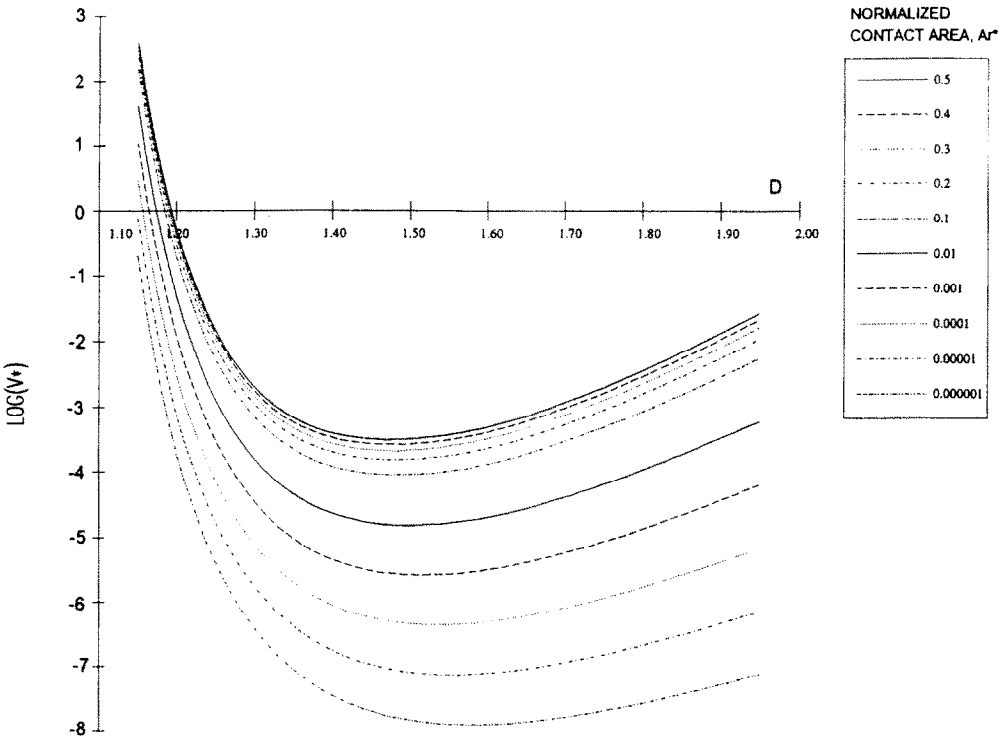

Fig. 8. Relation of normalized wear rate V^* to fractal dimension D with $\psi=0.01$, $G^*=10^{-9}$ and various values of A_r^*.

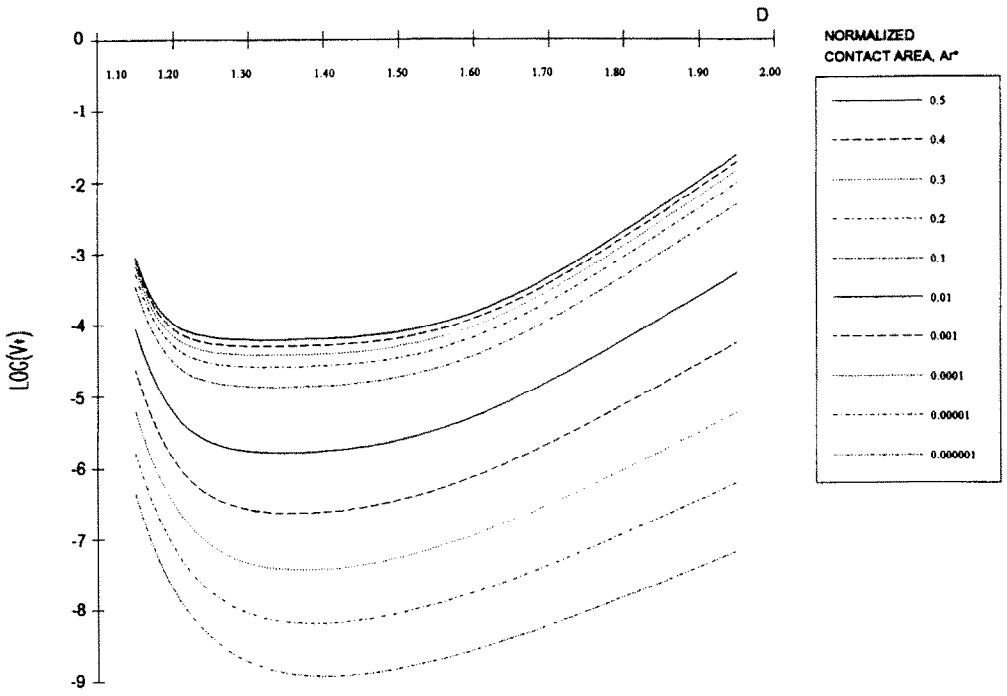

Fig. 9. Relation of normalized wear rate V^* to fractal dimension D with $\psi=0.1$, $G^*=10^{-9}$ and various values of A_r^*.

30 min, the fractal dimensions increased from their initial values. This is referred to as the fractal dimension enhancement stage in the figure. Apparently, when the surfaces first came into contact, the fresh and sharp layers of surfaces were removed; the surfaces became smoother and the surface contact support ability increased. After this stage, from the 30th to the 120th min, D increased slightly but maintained an overall balance. This is referred to as the fractal dimension balance stage. After 120 min D decreased greatly as the process continued. This is called the fractal dimension descent stage. This implies that the contact

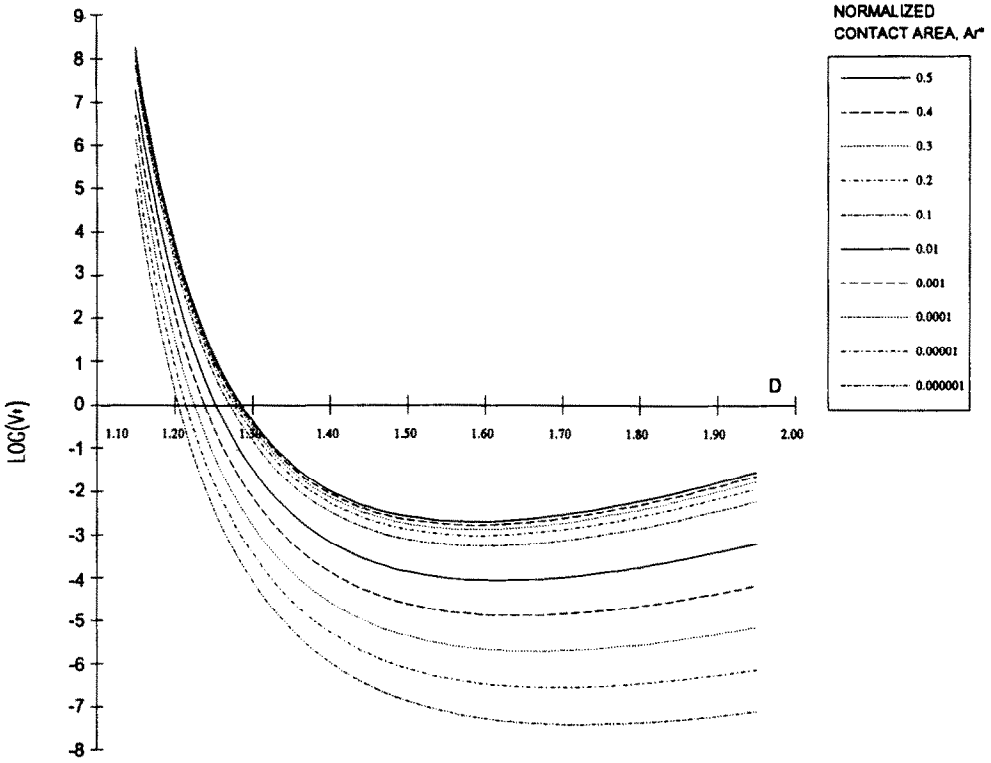

Fig. 10. Relation of normalized wear rate V^* to fractal dimension D with $\psi=0.001$, $G^*=10^{-9}$ and various values of A_r^*.

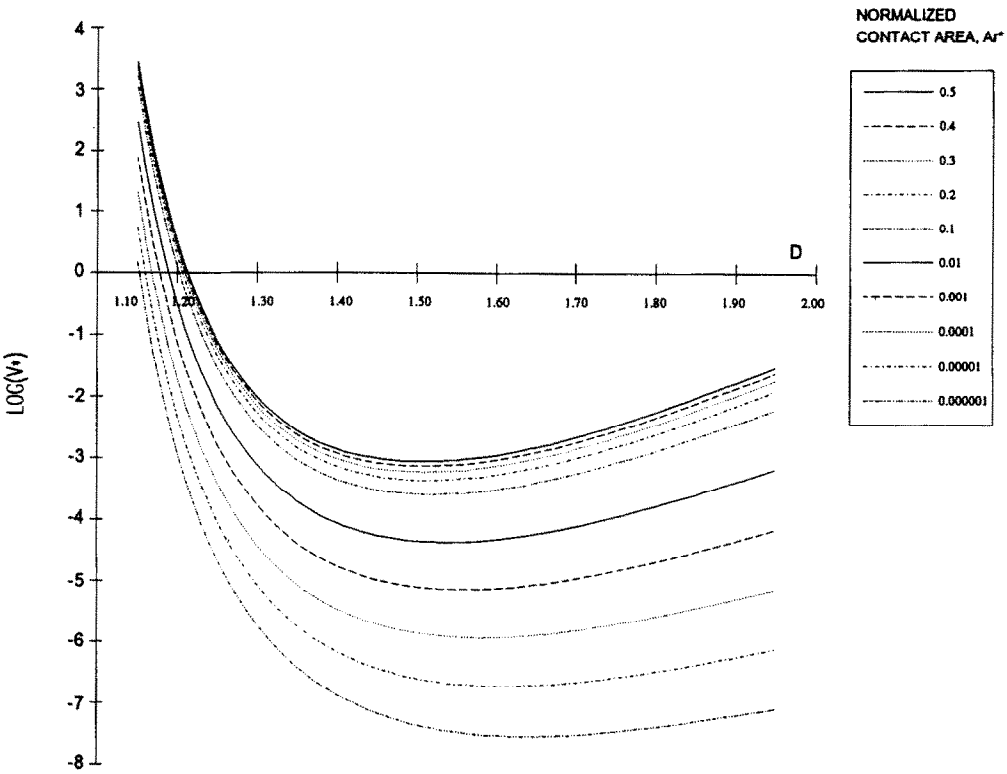

Fig. 11. Relation of normalized wear rate V^* to fractal dimension D with $G^*=10^{-8}$, $\psi=0.01$ and various values of A_r^*.

support ability of the surfaces becomes poorer and poorer because the surfaces become rougher and rougher. Comparing Fig. 13 with Fig. 14 we see that the three stages of wear rate correlate with the three stages of fractal dimension fairly well. This suggests that fractal dimension can be used to monitor the wear

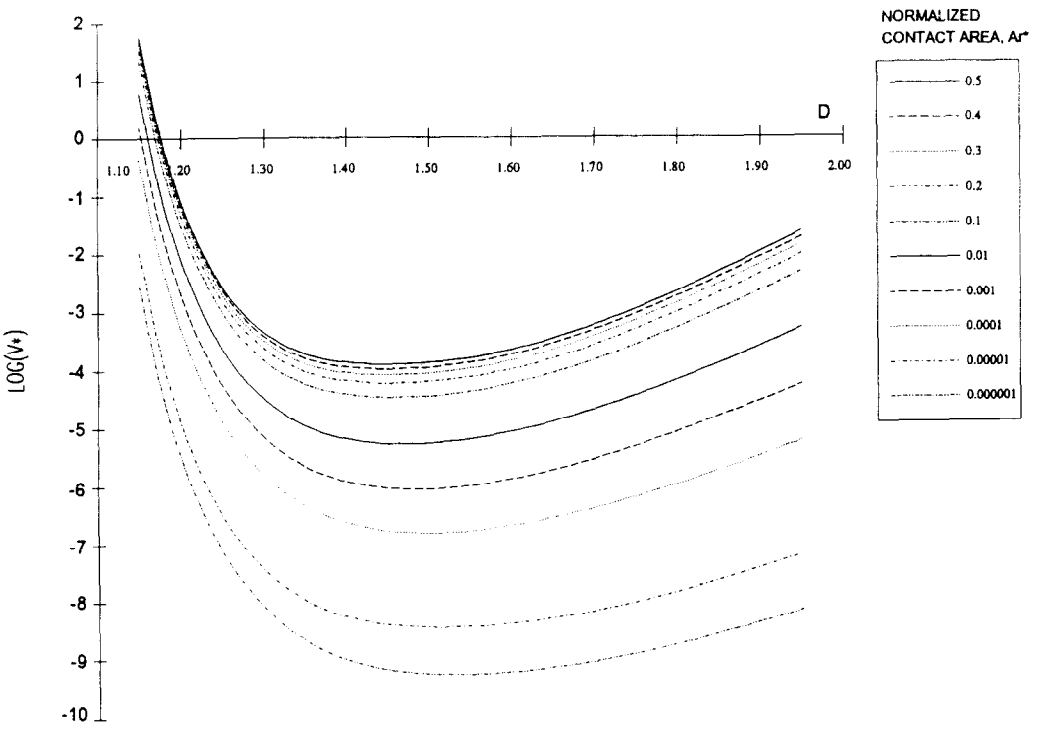

Fig. 12. Relation of normalized wear rate V^* to fractal dimension D with $G^*=10^{-10}$, $\psi=0.01$ and various values of A_r^*.

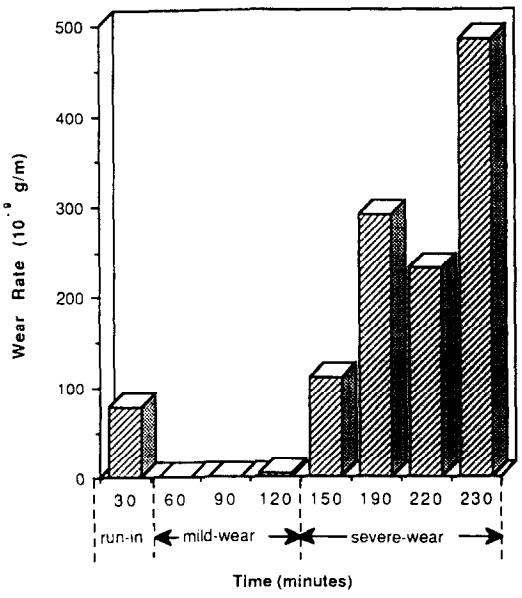

Fig. 13. The three stages of wear rate.

process. The same observations hold for the other three pairs of wear components.

From the above wear-testing process some parameter values for the roller were obtained as follows: $\mu=0.06$, $\psi=0.0034$, $G^*=65\times10^{-9}$ (average value for the whole process), $K_e=10^{-4}$ and $K_p=0.1$. To examine the validity

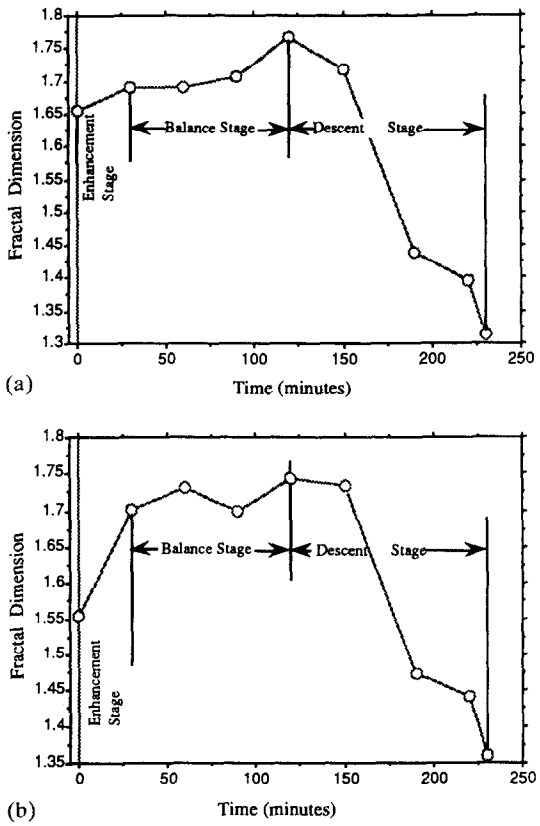

Fig. 14. The three stages of variations in the fractal dimensions of (a) a roller and (b) a shoe.

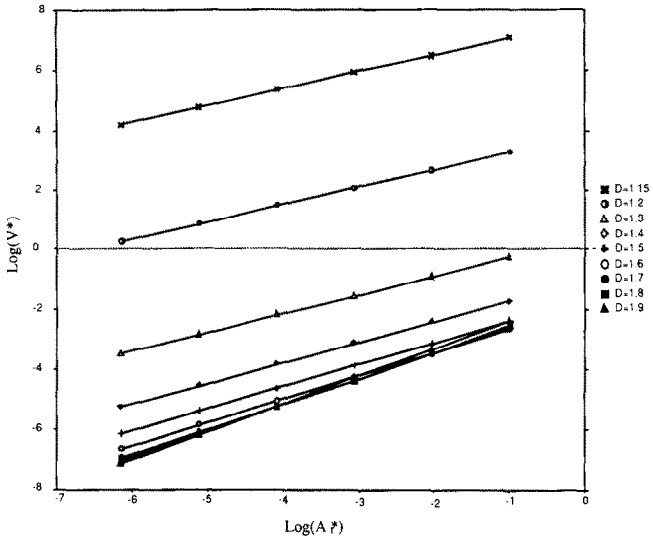

Fig. 15. The model results based on experimentally determined parameters.

of our model, these parameter values are used in eqn. (23) and the wear prediction graph is plotted in Fig. 15. From the figure it can be seen that the optimum fractal dimension for this particular wear process is around 1.7. This implies that $D=1.7$ is a change point of the wear rate, *i.e.*, if D is less than 1.7, V^* decreases with increasing D and, if D is larger than 1.7, V^* increases with increasing D. With the relation between V^* and D in Fig. 15, we see that the overall wear rate in Fig. 13 can be correctly predicted by the measured fractal dimension in Fig. 14.

7. Conclusions

Fractal geometry has been successfully used to characterize surface topography and surface contact support ability [9(a), 9(b)], and to model surface contact mechanics [8]. In this paper we have shown that fractal geometry can also be used to analyze wear processes. Our fractal geometry model for wear prediction leads to results which are consistent with experimental observations. Using this model it has been found that there are two regions of D which have different wear rate behavior. In one region wear rate decreases greatly with increasing D, and in the second region wear rate increases slightly with increasing D. We have explained these phenomena by using surface contact support ability and sharpness of asperities. Our model also predicts that wear rate increases monotonically as scale amplitude G increases or as material constant ψ decreases. Since there is a direct relation between G and topothesy L, the model provides a convenient means for using fractal parameters D and L to predict wear rates.

Based on the model we have found that there is a relationship between wear rate and true contact area under static loading as $V_r \propto A_r^{m(D)}$, with $m(D)$ between 0.5 and 1. This estimation is consistent with Archard's proposed relations $V_r \propto A_r$ for purely plastic deformation and $V_r \propto A_r^{2/3}$ for purely elastic deformation. Our model gives a general and practical expression for V_r and A_r in terms of surface fractal properties.

The optimum fractal dimension, corresponding to the minimum wear rate in a wear process, was derived by using the wear prediction model. It has been found that the optimum fractal dimension is determined by A_r, ψ and G. In ordinary cases a surface used in engineering practice has the optimum fractal dimension around 1.5, and this value shifts with changes in the three key parameters. When A_r or ψ increases, the optimum D decreases, but when G increases, the optimum D increases. Our optimum fractal dimension study provides useful information about how to prepare surfaces for wear reduction.

The results of wear testing tend to support our wear prediction model which leads to the conclusion that our fractal approach has considerable potential for the analysis of wear.

Acknowledgments

We wish to thank the referees for their penetrating comments that were instrumental in the improvement on the original draft of our paper.

References

1 J. A. Greenwood and J. H. Tripp, The contact of two nominally flat rough surfaces, *Proc. Inst. Mech. Eng., 185* (1970–1971) 625–633.
2 J. J. Gagnepain and C. Roques-Carmes, Fractal approach to two-dimensional and three-dimensional surface roughness, *Wear, 109* (1986) 119–126.
3 F. F. Ling, Fractals, engineering surfaces and tribology, *Wear, 136* (1990) 141–156.
4 A. Majumdar and B. Bhushan, Role of fractal geometry in roughness characterization and contact mechanics of surfaces, *ASME J. Tribol., 112* (1990) 205–216.
5 B. B. Mandelbrot, *The Fractal Geometry of Nature*, Freeman, New York, 1982.
6 H. O. Peitgen and D. Saupe, *The Science of Fractal Images*, Springer, New York, 1988.
7 B. H. Kaye, *A Random Walk Through Fractal Dimensions*, VCH, New York, 1989.
8 A. Majumdar and B. Bhushan, Fractal model of elastic–plastic contact between rough surfaces, *ASME J. Tribol., 113* (1991) 1–11.
9 (a) G. Y. Zhou, Statistical, random and fractal characterizations of surface topography with engineering applications, *Ph.D. Dissertation*, New Jersey Institute of Technology, Newark, NJ, 1992.

(b) G. Y. Zhou, M. C. Leu and D. Blackmore, Fractal characterization of surface topography and implementation in surface contact, *ASME J. Tribol.*, submitted for publication.
10 B. B. Mandelbrot, Self-affine fractals and fractal dimension, *Phys. Scr., 32* (1985) 257–260.
11 B. B. Mandelbrot, D. E. Passoja and A. J. Paullay, Fractal character of fracture surfaces of metals, *Nature (London),* (1984) 1571–1572.
12 M. V. Berry, Diffractals, *Physica A, 12* (1978) 781–797.
13 A. Thomas and T. R. Thomas, Digital analysis of very small scale surface roughness, *J. Wave–Mater. Interaction, 3* (4) (1988) 341–350.
14 J. F. Archard, Wear theory and mechanics, in M. B. Peterson and W. O. Winer (eds.), *Wear Control Handbook,* American Society of Mechanical Engineers, New York, 1980.
15 J. Korcak, Deux types fondamentaux de distribution statistique, *Bull. Inst. Stat., 3* (1938) 295–299.
16 M. V. Berry and Z. V. Lewis, On the Weierstrass–Mandelbrot fractal function, *Proc. R. Soc. London, Ser. A, 370* (1980) 459–484.
17 J. F. Archard, Contact and rubbing of a flat surface, *Appl. Phys., 24* (1953) 981–988.
18 M. M. Kruschov, Resistance of metals to wear by abrasion; related to hardness, *Proc. Conf. on Lubrication and Wear,* Institution of Mechanical Engineers, London, 1957, pp. 655–659.
19 N. P. Suh, The delamination theory of wear, *Wear, 25* (1973) 111–124.
20 T. A. Stolarski, A probabilistic approach to wear prediction, *J. Phys. D, 24* (1990) 1143–1149.
21 S. Wu and H. S. Cheng, A sliding wear model for partial-EHL contacts, *ASME J. Tribol., 113* (1991) 134–141.
22 D. Tabor, Junction growth in metallic friction: the role of combined stresses and surface contamination, *Proc. R. Soc. London, Ser. A, 251* (1959) 378–389.
23 R. Dubrovsky and I.-T. Shih, Development of the computer controlled seizure testing methodology, in *New Materials Approach to Tribology: Theory and Applications, Materials Research Society Symp. Proc.,* Vol. 140, Materials Research Society, Philadelphia, PA, 1988.
24 G. Y. Zhou, M. C. Leu and S. X. Dong, Measurement and assessment of topography of machined surfaces, in *Microstructural Evolution in Metal Processing, ASME Winter Meet.,* American Society of Mechanical Engineers, 1990, pp. 89–100.